Comparative Study of the Influence of Straight and Modified-Tip Rotor Blades on Loads and Control Response

Session subject – Dynamics

M. Rohin Kumar, Senior Project Associate, kumar.rohin@gmail.com
and
C. Venkatesan, Professor and Head, cven@iitk.ac.in
Department of Aerospace Engineering,
Indian Institute of Technology, Kanpur, India, 208016

Abstract

For performance improvement and noise reduction, swept and anhedral tips have been incorporated in *advanced geometry* rotor blades. While there are aerodynamic benefits to these advanced tip geometries, they come at the cost of complicated structural design and weight penalties. The effect of these tip shapes on loads, vibration and aeroelastic response are also unclear. In this study, a comprehensive helicopter aeroelastic analysis which includes rotor-fuselage coupling shall be, briefly, described and the analysis results for rotor blades with straight tip, tip-sweep and tip-anhedral shall be presented and compared. The helicopter modeled is a conventional one with a hingeless single main rotor and single tail rotor. The blade undergoes flap, lag, torsion and axial deformations. Aerodynamic model includes 3-state Peters-He dynamic wake theory for inflow and the *modified* ONERA dynamic stall theory for airloads calculations. The complete 6-dof nonlinear equilibrium equations are solved for analyzing any general flight condition. Response to pilot control inputs is determined by integrating the full set of nonlinear equations of motion with respect to time. The effects of tip-sweep and tip-anhedral on loads and vehicle response to pilot inputs shall be presented.

NOTATION

a	:	Torque offset of the rotor blade
g	:	Acceleration due to gravity (= 9.81 m^2/s)
I_{xx}, I_{yy}, I_{zz}, I_{xz}	:	Aircraft mass moments of inertia about body axes at the c.g
L, M, N	:	Components of total moments along body axes at the c.g
m	:	Mass of the helicopter, kg
p, q, r	:	Angular velocities along body axes at the c.g
u, v, w	:	Velocity components along body axes at the c.g
X, Y, Z	:	Components of the total forces along body axes at the c.g
β_d	:	Pre-droop angle of rotor blade
β_p	:	Pre-cone angle of rotor blade
β_s	:	Pre-sweep angle of rotor blade
θ_0	:	Main rotor collective
θ_{0t}	:	Tail rotor collective
θ_{1C}	:	Lateral cyclic
θ_{1S}	:	Longitudinal cyclic
μ	:	Advance ratio
ρ	:	Density of the blade, kg/m^3
Θ	:	Fuselage pitch attitude
Λ_a	:	Tip-anhedral angle
Λ_s	:	Tip-sweep angle
Φ	:	Fuselage roll attitude
Ψ	:	Rotor blade azimuth angle
Ω	:	Rotational speed of the rotor blade, rpm
Ω_a	:	Turn rate of vehicle, rad/s

1. INTRODUCTION

For performance improvement and noise reduction, *advanced geometry* rotor blades have incorporated swept and anhedral tips [1]. Swept tips are introduced in rotor blades, usually, to delay compressibility effects, to reduce *Mach tuck* and to improve performance, in general. Likewise, tip anhedral is introduced to prevent tip vortex - blade interaction resulting in a more uniform angle-of-attack distribution and, hence, better performance. While there are aerodynamic benefits to these advanced tip geometries, they come at the cost of complicated structural design and weight penalties. The effect of these tip shapes on loads, vibration and aeroelastic response are also unclear. Hence, it has become necessary to study the effects of these *advanced geometry* blades on the aeroelastic behavior of the rotor system. Swept and anhedral tips influence blade dynamics because they are located at regions of high dynamic pressure and relatively large elastic displacements. Rotor blades with sweep and anhedral at the blade-tip region experience bending torsion and bending-axial coupling effects. Aeroelastic analyses of advanced geometry blades with tip sweep and anhedral can be found in [2, 3]. Studies of composite rotor blades with advanced geometry can be found in [4 – 6]. These analyses have included Panda's [7] general nonlinear transformation and constraint relations at the junction between two blade elements joined at an angle to each other. These transformations have included nonlinearities which were found to be important, especially for large sweep angles.

In this paper, the results of a comprehensive helicopter aeroelastic analysis for rotor blades with straight tip, tip-sweep and tip-anhedral are compared. The effects of tip-sweep and tip-anhedral on loads and vehicle response to pilot inputs are presented.

2. MODELING

2.1 Blade Structural Model

The structural and the aerodynamics models used in the helicopter aeroelastic analysis have been described in [8-10]. Hence, only a brief outline is given here without much mathematical details.

For the structural model, an elastic rotating beam with constant angular velocity Ω was considered. Blade sweep, precone, predroop, pretwist, root offset and torque offset are included in the model (Fig. 1). The beam consists of a straight portion and a tip with sweep and anhedral angles relative to the straight portion. By convention, backward sweep and upward dihedral angles have been taken as positive. The cross-section of the blade has a general shape with distinct shear center and center of mass.

The nonlinear equations of motion and the corresponding finite element matrices were derived for each beam element using Hamilton's principle. The blade was modeled by a series of straight beam finite elements along the elastic axis of the blade. Two finite elements at the tip were used to model the sweep and anhedral. Each finite element in the tip can be given a sweep angle and/or anhedral angle independent of the other. Each beam element consists of two end nodes and one internal node at its mid-point, resulting in 14 degrees of freedom representing 4 lag, 4 flap, 3 torsional and 3 axial deformations. Cubic Hermite interpolation polynomials are used for the bending displacement, while quadratic Lagrangian interpolation polynomials are used for torsional rotation and axial deflections. Applying Hamilton's principle to each finite element results in a discretised form of the equations of motion.

2.2 Aerodynamic Model

The aerodynamic model involves the evaluation of inflow at various locations on the rotor disc and the evaluation of sectional aerodynamic loads on the rotor blade. For the purpose of this paper, a 3-state Peters-He dynamic wake model [11] for inflow and the ONERA dynamic stall model [12] for loads are discussed. Both these models, by virtue of their being formulated as a set of differential equations are very suitable for aeroelastic calculations.

The Peters-He dynamic wake model is a compact formulation with multiple states that allow variation of the inflow in the radial as well as azimuthal directions. While the model allows for multiple states, for the analysis in this paper, three states were used. The ONERA model describes the unsteady airfoil behaviour in both attached flow and separated flow using a set of nonlinear differential equations. In the unstalled region, it is identical to Theodorsen's unsteady aerodynamic theory except that the lift deficiency function C(*k)* is approximated by a first order rational approximation. The study in [13] concluded that replacing the first order rational approximation by a second order approximation results in a more accurate *modified* ONERA dynamic stall model, which shall be used in the present analysis.

2.3 Flight Dynamics

The equations of motion for the six fuselage degrees of freedom are assembled by applying Newton's laws of motion relating the applied forces and moments to the resulting translational and rotational

accelerations. These are given by equations (1) – (6) below.

$$(1)\quad \dot{u} = -(w_g q - v_g r) + \frac{X}{m} - g\sin\Theta$$

$$(2)\quad \dot{v} = -(u_g r - w_g p) + \frac{Y}{m} - g\cos\Theta\sin\Phi$$

$$(3)\quad \dot{w} = -(v_g p - u_g q) + \frac{Z}{m} - g\cos\Theta\sin\Phi$$

$$(4)\quad I_{xx}\dot{p} = (I_{yy} - I_{zz})qr + I_{xz}(\dot{r} + pq) + L$$

$$(5)\quad I_{yy}\dot{q} = (I_{zz} - I_{xx})rp + I_{xz}(r^2 - p^2) + M$$

$$(6)\quad I_{zz}\dot{r} = (I_{xx} - I_{yy})pq + I_{xz}(\dot{p} - qr) + N$$

The kinematic equations (7) – (9) give the relationship between the time rate of change of the Euler angles and the fuselage angular velocities in the body axes system.

$$(7)\quad \dot{\Phi} = p + q\sin\Phi\tan\Theta + r\cos\Phi\tan\Theta$$

$$(8)\quad \dot{\Theta} = q\cos\Phi - r\sin\Phi$$

$$(9)\quad \dot{\Psi} = q\sin\Phi\sec\Theta + r\cos\Phi\sec\Theta$$

The nonlinear trim equations are obtained from the above equations by setting the rate of change of magnitude of the velocity vector to zero.

3. SOLUTION PROCEDURE

For structural dynamics, the rotor blade was modeled using finite elements, with each element having 14 degrees of freedom. Modal coordinate transformation was used to reduce the total number of degrees of freedom. Eight modes comprising of the two lag, four flap, one torsion and one axial modes were used in the modal transformation. The aerodynamic loads were calculated at 15 equidistant stations on the rotor blades. The trim equations comprise the complete nonlinear vehicle force and moment equilibrium equations. The trim algorithm [9,10] was implemented as a C++ program using the open-source *GSL* [14] as the math library. The differential equations were solved using the Runge-Kutta method while the non-linear algebraic trim equations are solved using the Newton-Raphson method. The program outputs inflow over the rotor, hub loads, blade response, blade sectional loads, blade shear and bending moments, pilot inputs and the vehicle attitudes.

The helicopter response to pilot control inputs is determined by integrating the full set of nonlinear equations of motion (Eqs. (1) – (9)) with respect to time after evaluating the blade and hub loads at every time step. The helicopter which is flying in level, forward trim condition is subjected to a step-input in the lateral cyclic and longitudinal cyclic angle, one at a time, for 5 seconds. The response of the helicopter to these disturbances is studied in terms of its translational and angular velocities. The flow chart for control response procedure is shown in Fig. 2.

The vehicle and blade properties are given in Table 1. The structural dynamics formulation was validated [8] with the *University of Maryland* vacuum chamber experiments [6] and was also compared with *RCAS* results [15] for the same set of experimental data. The aeroelastic formulation was also validated in [8,16] with flight test data.

4. RESULTS

Results pertaining to the influence of tip-sweep and tip-anhedral on rotor structural dynamics, helicopter trim and control response are discussed here. Sweep or anhedral is given over the outer 10% of the overall span of the rotor blade. The blades have the same property in every other aspect. Results of two tip-sweep cases (15 deg and 30 deg) and two tip-anhedral/dihedral cases (-10 deg and 10 deg) are compared with those of the straight blade case. It is to be noted that tip-anhedral is denoted by negative angle and tip-dihedral by positive angle.

4.1 Effect of Swept Tip

It is known that tip-sweep effect on blade frequencies is mostly seen in the torsion and higher bending modes. It is also known that tip-sweep introduces torsion-bending coupling in the mode shapes of the rotor blade.

Tip-sweep influences the aerodynamic and structural forces acting on the blade. These, in turn, influence the pilot control settings for trim. Figure 3 shows the variation of trim angles with forward speed for different tip-sweep angles. It is seen that when compared to the straight blade case, the main rotor collective angles required to trim the vehicle decreases with increase in tip-sweep angle. The lateral and the longitudinal cyclic angles decrease slightly with increase in tip-sweep. The reason for this, as will be seen later, is the reduction in the torsion experienced by the rotor blade with tip-sweep as compared to the straight blade.

Figure 4 shows the variation of the mean and 1/rev elastic twist at 0.70R with forward speed. It is seen that there is a clear reduction in the amplitude of the mean with increase in tip-sweep. This reduction in the steady elastic twist results in a reduced main rotor collective requirement in trim as was seen in the previous figure. This has also been observed in [1]. Figure 5 shows the effect of tip-sweep on the blade response at 0.70R with time

(azimuth) for a forward speed of μ = 0.30. Data for the straight blade is represented by the line with a star symbol, while those of blades with 15deg and 30deg tip-sweeps are represented by lines with filled-circle symbol and hollow-circle symbol, respectively. This is the convention followed for the next few figures. While the flap response increases very slightly with tip-sweep, there is a clear reduction in lag with increase in tip-sweep. The elastic twist or torsion reduces both in mean value and the amplitude with increase in tip-sweep. Harmonic content of the torsion response is seen to increase with increase in tip-sweep. The elastic twist is also seen to reduce in the advancing side of the rotor. This allows for a much higher collective angle.

Next, the loads on the helicopter rotor blade with varying tip-sweeps are plotted for a forward speed of μ = 0.30. The loads are expected to be affected because of the change in local velocity normal to the blade at the tip due to the introduction of sweep. Another factor affecting the loads is the offset of the aerodynamic center from the elastic axis. Lift, drag and the torsional moment are given about the elastic axis of the straight portion of the blade. For the inboard sections, there is only a slight effect of tip-sweep on the sectional loads, mostly in the advancing side. These can be seen in Ref. 18. Figure 6 shows the effect of tip-sweep on sectional lift, drag and torsional moment for an outboard section (0.95R). The effect of tip-sweep is seen less on the sectional lift and drag and mostly on the sectional pitching moment (Fig. 6c). At 0.95R, there is a drastic reduction in the pitching moment with increase in tip-sweep. This is because of the aerodynamic center offset from the elastic axis at the tip. This can be beneficial as it helps in the reduction of the pitch link loads.

Figure 7 shows the effect of tip-sweep on the blade root loads. The plots show a reduction in the peak-to-peak values of the x-component (axial) and the y- component of the root shear force. There is hardly any change in the z-component of the root shear force. Similarly, there is a clear reduction in the peak-to-peak values of the root torsional and root lag moments while the root flap moment hardly shows any change with increase in tip-sweep.

Figure 8 shows the effect of tip-sweep on the hub loads. The variation of the three force and three moment components of the hub loads with the azimuth are plotted for the three blade configurations. There is no clear trend but, overall, the peak-to-peak values of both the forces and moments seem to be increasing with increase in tip-sweep. This means that the vibratory loads transferred to the fuselage from the rotor increase with increase in tip-sweep.

4.2 Effect of Tip Anhedral

It is known that the effect of tip-anhedral/dihedral on the bending and torsional frequencies is very small. Their effect is, mostly, seen in the axial mode whose frequency increase with the introduction of tip-anhedral/dihedral. Like tip-sweep, tip-anhedral/dihedral also introduce torsion-bending coupling.

Like tip-sweep, tip-anhedral/dihedral also influence the aerodynamic and structural forces acting on the blade resulting in a change to the pilot control settings for trim. Figure 9 shows the variation of trim angles with forward speed for tip-anhedral/dihedral angles. It is seen that when compared to the straight blade case, the main rotor collective angles required to trim the vehicle slightly increase for both tip-anhedral and tip-dihedral cases. The lateral cyclic decreases for the tip-anhedral case and increases for the tip-dihedral case. Tip-anhedral and tip-dihedral introduce opposite variations in the angle-of-attack in the front and aft regions of the rotor. This is the reason for their opposite effects on the lateral cyclic. The longitudinal cyclic angle shows a slight decrease with increase in tip-dihedral. With tip-anhedral, the longitudinal cyclic is almost the same as the straight blade.

Figure 10 shows the variation of the mean and 1/rev elastic twist at 0.70R with forward speed. It is seen that there is a small, reduction in the amplitude of the mean for both tip-anhedral and tip-dihedral cases. This reduction in the steady elastic twist is in contrast to the increase in main rotor collective requirement in trim as was seen in the previous figure. Figure 11 shows the effect of tip-anhedral/dihedral on the blade response at 0.70R with time (azimuth) for a forward speed of μ = 0.30. Data for the straight blade is represented by the line with a star symbol, while those of blades with -10deg tip-anhedral and 10deg tip-dihedral are represented by lines with filled-circle symbol and hollow-circle symbol, respectively. This is the convention followed for the next few figures. The flap response decreases with the introduction of tip-anhedral/dihedral. This could be attributed to centrifugal stiffening. The peak-to-peak lag amplitude is seen to reduce with addition of tip-anhedral/dihedral. The mean amplitude of torsion reduces when tip-anhedral/dihedral is introduced.

Next, the loads on the helicopter rotor blade with varying tip-anhedral are plotted for a forward speed of μ = 0.30. The loads are expected to be affected because of the offset of the center of gravity near the tip. The effect of tip-anhedral/dihedral on sectional lift, drag and torsional moment is mostly seen in the outboard section (Fig. 12). The results of

the inboard sections can be seen in Ref. 16. The peak-to-peak amplitude of the sectional lift is seen to increase for rotor blade with tip-anhedral/dihedral. In the case of sectional drag, the outboard section (0.95R) experiences a drastic increase in drag, especially on the retreating side. Regarding sectional pitching moment, the peak-to-peak amplitude of the pitching moment is decreased in the case of tip-anhedral and increased in the case of tip-dihedral.

Comparing Fig. 12 with Fig. 6, it is seen that tip-anhedral/dihedral tend to affect the loads more than tip-sweep, especially in the outboard sections. An interesting observation in Figs. 12 is that at 0.95R, the sectional lift and drag at azimuth locations 90deg and 270deg are not affected by tip-anhedral/dihedral. In the case of sectional pitching moments, these 'invariant' points are around 65deg and 210deg.

Figure 13 shows the effect of tip-anhedral/dihedral on the blade root loads. The plots show a reduction in the peak-to-peak values of the x-component (axial) and the y-component of the root shear force. There is hardly any change in the z-component of the root shear force. Similarly, there is a clear reduction in the peak-to-peak values of the root torsional and root lag moments while the root flap moment hardly shows any change with addition of tip-anhedral/dihedral. In Fig. 13c, a small dip in magnitude is seen in the z-component of root shear for the blade with tip-dihedral in the fourth quadrant (circled in red). This is because of a large negative angle-of-attack in the reverse flow region of the blade. However, this phenomenon was not observed either in the straight blade or the blade with tip-anhedral and needs to be investigated further.

Figure 14 shows the effect of tip-anhedral/dihedral on the hub loads. The variation of the three force and three moment components of the hub loads with the azimuth are plotted for the three blade configurations. From the three force components, it is observed that addition of a tip-anhedral or a tip-dihedral results in an increase in either the mean of the force component or the peak-to-peak amplitude. This means that the vibratory loads transferred to the fuselage from the rotor is higher for blades with tip-anhedral/dihedral than for straight blades. The observation of additional harmonics in the hub thrust (Fig. 14c) for the blade with tip-dihedral is attributed to the large negative angle-of-attack in reverse flow region which was discussed earlier.

4.3 Control Response

Next, helicopter flight behaviour following pilot control inputs is analyzed. Detailed knowledge of the control response is essential for determining the flying qualities of a helicopter. In this section, the effects of addition of blade tip-sweep and tip-anhedral/dihedral on the rotor control response are studied.

Figure 15 shows the helicopter translational and angular velocity responses to a lateral cyclic step-input for $\mu = 0.30$. While the analysis was also carried out for hover and low speed forward flight, the effect of rotor blade tip-sweep and tip-anhedral/dihedral on the control response was found to be negligible.

Figure 15a shows the control response for rotor with straight blades. At $\mu = 0.30$, the pitch attitude of the helicopter is about -1deg and the roll attitude is about -2.5 deg. Among the translational velocity components, only the y-axis component changes in the first couple of seconds. It increases in the positive direction. Among the angular velocity components, the roll rate reaches a value of about -10deg/s in about 0.3 seconds (inset) and rises to about -40deg/s by 2.5 seconds. From Fig. 15b which is the case of rotor blade with 30deg tip-sweep, it is seen that there is hardly any effect of sweep on the control response. In case of blade with tip-anhedral (-10deg, Fig. 15c), it is seen that till about 2.5 seconds, the response is similar to the straight blade case. Beyond 2.5 seconds, the z-component of velocity, the pitch and roll rates all experience a change in direction from their values in the straight blade case. Figure 15d shows the control response in the case of rotor blade with tip-dihedral (10deg). The y- and z-components of the body velocity and the pitch and yaw rates show opposite trend as compared to the tip-anhedral case. Thus, at high forward speed, the lateral cyclic response is seen to be affected by tip-anhedral/dihedral but not by tip-sweep.

Figure 16 shows the response due a longitudinal cyclic step-input. From Fig. 16a (straight blade) and Fig. 16b (30deg tip-sweep), it is seen that there is only a slight effect of tip-sweep on the control response. Between the tip-anhedral (Fig. 16c) and tip-dihedral (Fig. 16d) cases, the tip-dihedral has the most effect on the control response. In this case, the directions of the roll and yaw rates are changed from those of the straight blade case.

5. CONCLUDING REMARKS

A comprehensive helicopter aeroelastic analysis which includes rotor-fuselage coupling has been formulated and validated for structural dynamics and trim. The effects of tip-sweep and tip-anhedral/dihedral on structural dynamics, trim and control response of the helicopter were studied. The main observations are:

1. Tip-sweep reduces the main rotor collective angle requirement for trim in forward flight.
2. Tip-sweep reduces the sectional pitching moment near the tip, thereby, reducing the pitch-link loads.
3. The peak-to-peak values of the hubloads increase with increase in tip-sweep. Thus the vibratory loads transferred to the fuselage from the rotor are also increased.
4. Tip-anhedral and tip-dihedral have opposite effects on the required lateral cyclic in trim.
5. Tip-anhedral/dihedral have a larger effect on the loads in the outboard region than tip-sweep.
6. As in the case of tip-sweep, vibratory loads transferred to the fuselage from the rotor are increased due to tip-anhedral/dihedral.
7. Lateral cyclic control response at high-speeds in forward flight is affected by tip-anhedral/dihedral but not by tip-sweep.

ACKNOWLEDGEMENT

The authors would like to thank *Hindustan Aeronautics Limited* for their support and funding of this work.

COPYRIGHT STATEMENT

REFERENCES

1. Yen, J.G., "Effects of Blade Tip Shape on Dynamics, Cost, Weight, Aerodynamic Performance, and Aeroelastic Response," *Journal of the American Helicopter Society*, Vol. 39, No. 4, October 1994.
2. Celi, R., and Friedmann, P. P., "Structural Optimization with Aeroelastic Constraints of Rotor Blades with Straight and Swept Tips," *AIAA Journal*, Vol. 28, No. 5, 1992.
3. Kim, K.C., and Chopra, I., "Aeroelastic Analysis of Swept, Anhedral, and Tapered Tip Rotor Blades," *Journal of the American Helicopter Society*, Vol. 37, No. 1, 1992.
4. Yuan, K.A., Friedmann, P.P. and Venkatesan, C., "A New Aeroelastic Model for Composite Rotor Blades with Straight and Swept Tips," *33rd AIAA Structural Dynamics & Materials Conference*, AIAA 92-2259, Dallas, Texas, April 1992.
5. Yuan, K.A., and Friedmann, P.P., "Aeroelasticity and Structural Optimization of Composite Helicopter Rotor Blades with Swept Tips," *NASA CR-4665*, 1995.
6. Epps, J.J., and Chandra, R., "The Natural Frequencies of Rotating Composite Beams with Tip Sweep," *Journal of the American Helicopter Society*, Vol. 41, No. 1, 1996.
7. Panda, B., "Assembly of Moderate-Rotation Finite Elements Used in Helicopter Rotor Dynamics," *Journal of the American Helicopter Society*, Vol. 32, No.4, 1987.
8. Rohin Kumar, M., and Venkatesan, C., "Structural Dynamic Analysis of Helicopter Rotor Blades with Advanced Geometry Tip Shapes," *XVII NASAS*, IIT Kanpur, India, September 2011.
9. Rohin Kumar, M., and Venkatesan, C., "Rotorcraft Aeroelastic Analysis using Dynamic Wake/Dynamic Stall Models and its Validation," *Proceedings of IFASD 2013*, Bristol, UK, June 2013.
10. Rohin Kumar, M., and Venkatesan, C., "Aeroelastic Analysis of a Helicopter in Steady Maneuver using Dynamic Wake/Dynamic Stall Models," *European Rotorcraft Forum*, Moscow, Russia, September 2013.
11. He, Cheng Jian., "Development and Application of a Generalized Dynamic Wake Theory for Lifting Rotors," *Ph.D Dissertation*, Georgia Institute of Technology, July 1989.
12. Petot, D., "Differential Equation Modeling of Dynamic Stall", *La Reserche Aerospatiale*, Paper No. 1989-5, 1989.
13. Laxman, V., and Venkatesan, C., "Chaotic Response of an Airfoil due to Structural Coupling and Dynamic Stall," *AIAA Journal*, Vol. 45, Jan. 2007.
14. GSL – GNU Scientific Library, URL: http://www.gnu.org/software/gsl/
15. Hopkins, A.S., and Ormiston, R.A., "An Examination of Selected Problems in Rotor Blade Structural Mechanics and Dynamics," *Proceedings of the American Helicopter Society 59th Annual Forum,* Phoenix, Arizona, May 2003.
16. Rohin Kumar, M., "Comprehensive Aeroelastic and Flight Dynamic Formulation for the Prediction of Loads and Control Response of a Helicopter in General Maneuvering Flight," *PhD Thesis*, Department of Aerospace Engineering, Indian Institute of Technology, February 2014.

Table 1 Vehicle and blade properties

Parameter	Symbol	Value	Units
Air density	ρ	0.954	kg/m^3
Main rotor			
Number of blades	N	4	
Non-dimensional blade chord	c/R	0.0757	
Solidity ratio	σ	0.09646	
Weight coefficient	C_W	0.00734	
Pre-Twist		-12	degrees
Lift curve slope	$c_{l\alpha}$	5.73	
Profile drag coefficient	c_{d0}	0.01	
Lock number	γ	6.4	
Torque offset	*a*	0.0015	
Predroop	β_d	2.5	degrees
Modal frequencies of rotor blade			
Lag		0.71, 5.30	
Flap		1.09, 2.88, 5.01, 7.57	
Torsion		4.37	
Axial		33.36	
Vehicle			
Equivalent flat plate area		0.0131	
Parasite drag coefficient		1	

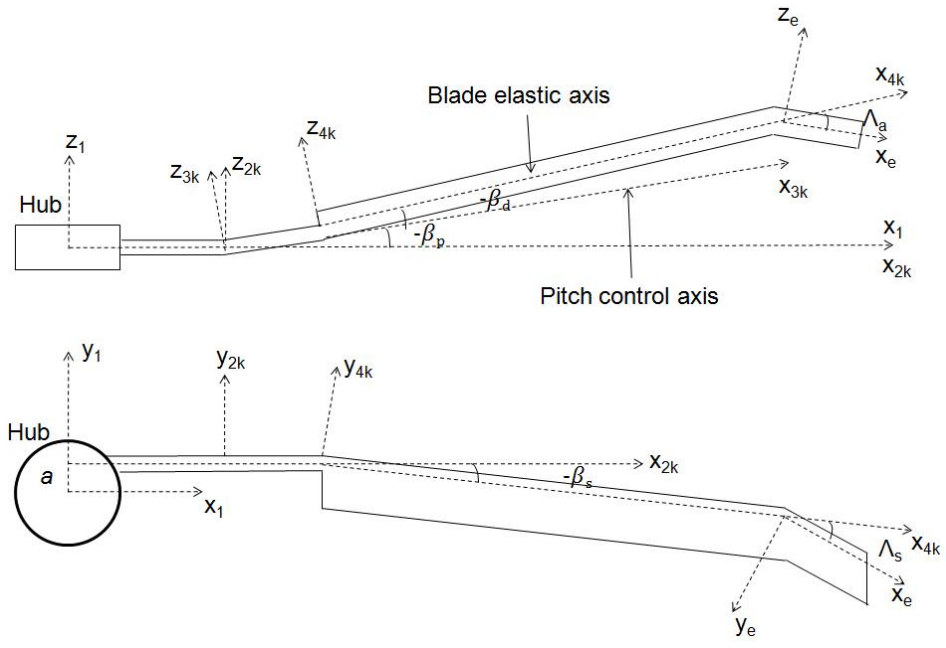

Fig. 1 Blade coordinate systems (Side and Top views)

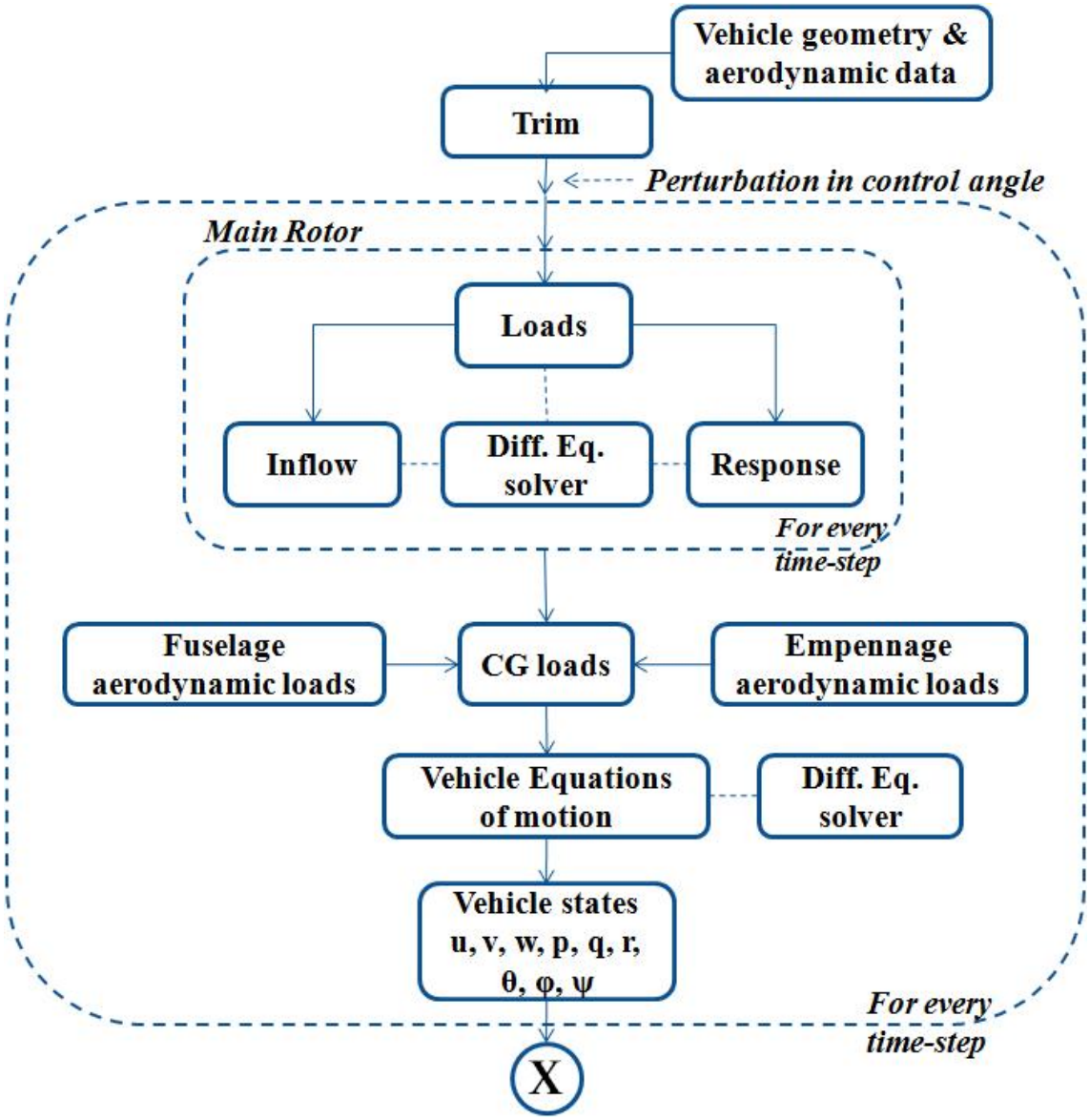

Fig. 2 Flowchart for helicopter response to pilot control input

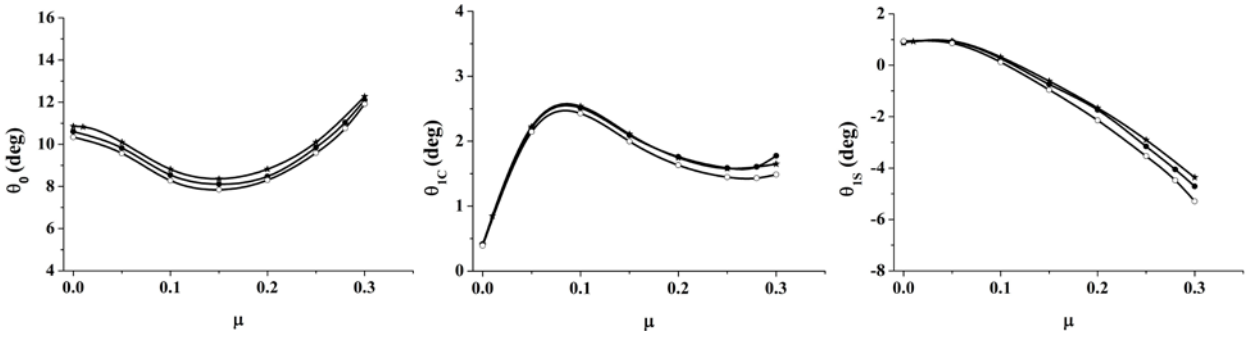

Fig. 3 Effect of tip-sweep on trim variables

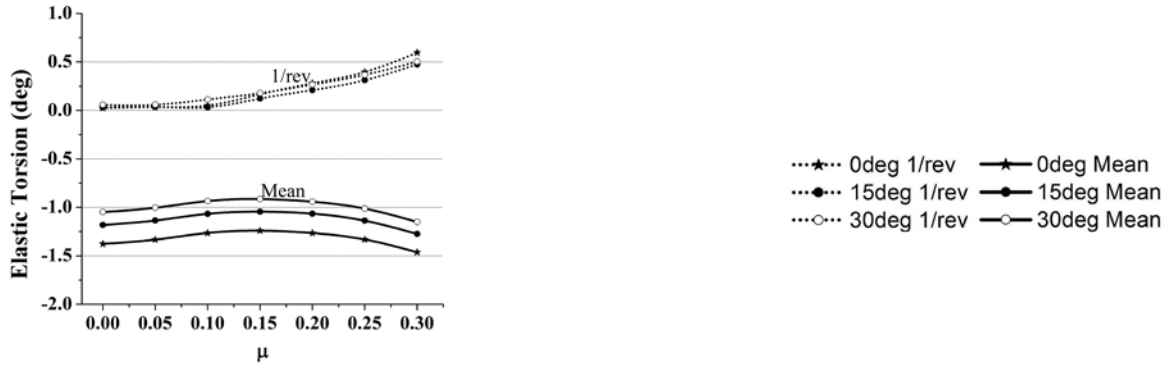

Fig. 4 Blade elastic twist at 0.70R

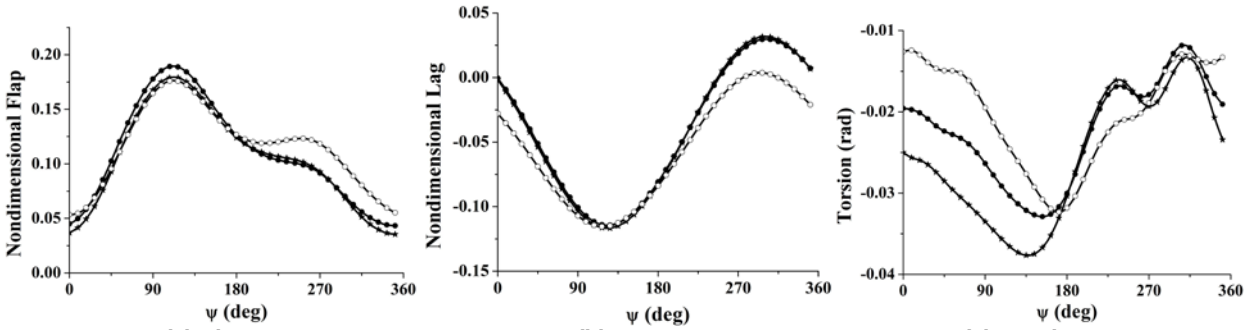

Fig. 5 Tip Response at 0.70R for μ = 0.30

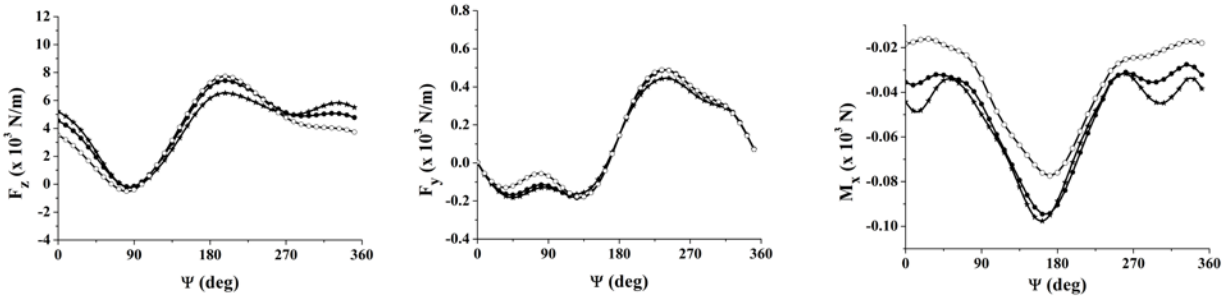

Fig. 6 Sectional loads @ 0.95R at μ = 0.30

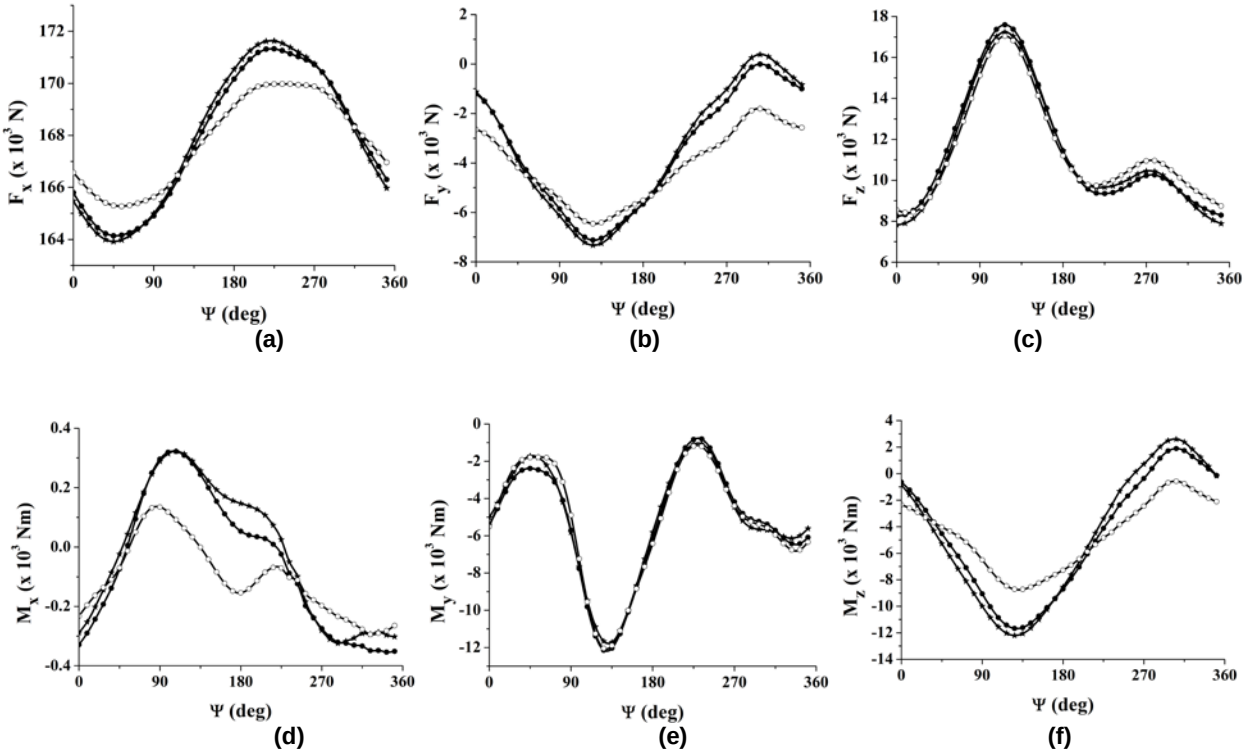

Fig. 7 Root forces and moments at μ = 0.30

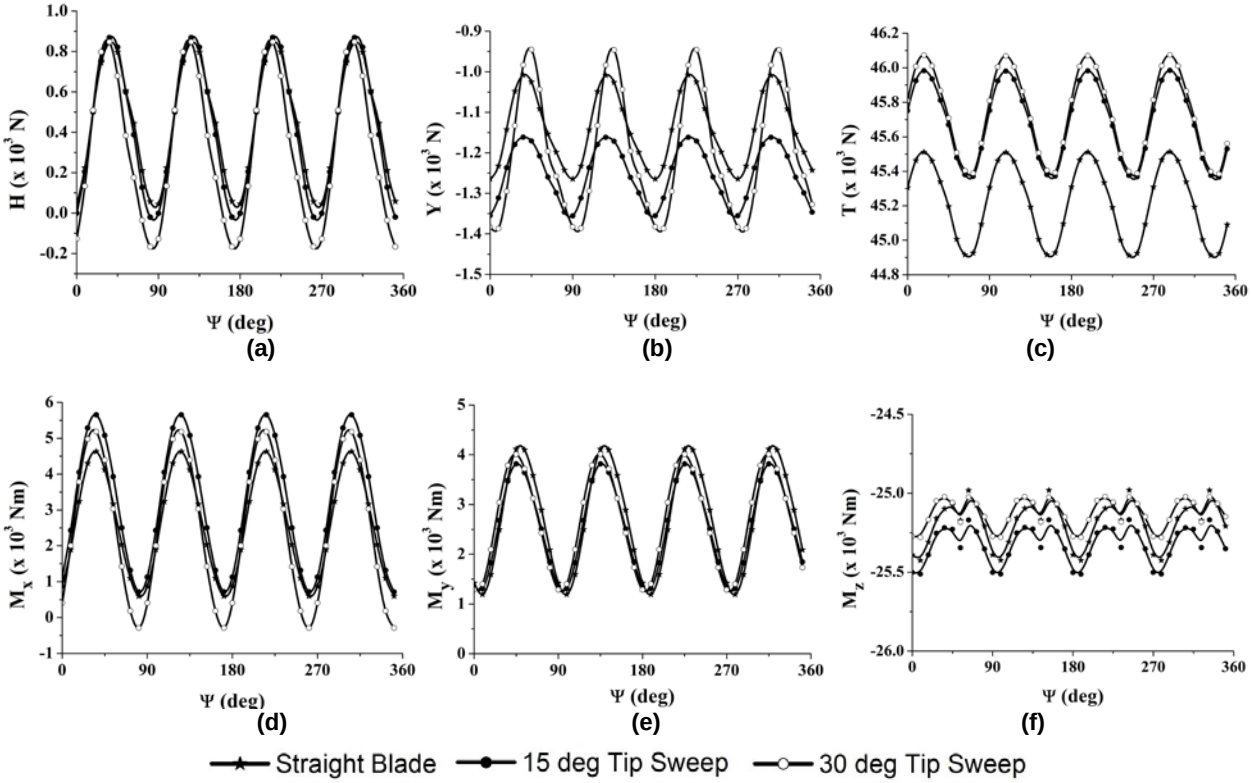

Fig. 8 Hub forces and moments at μ = 0.30

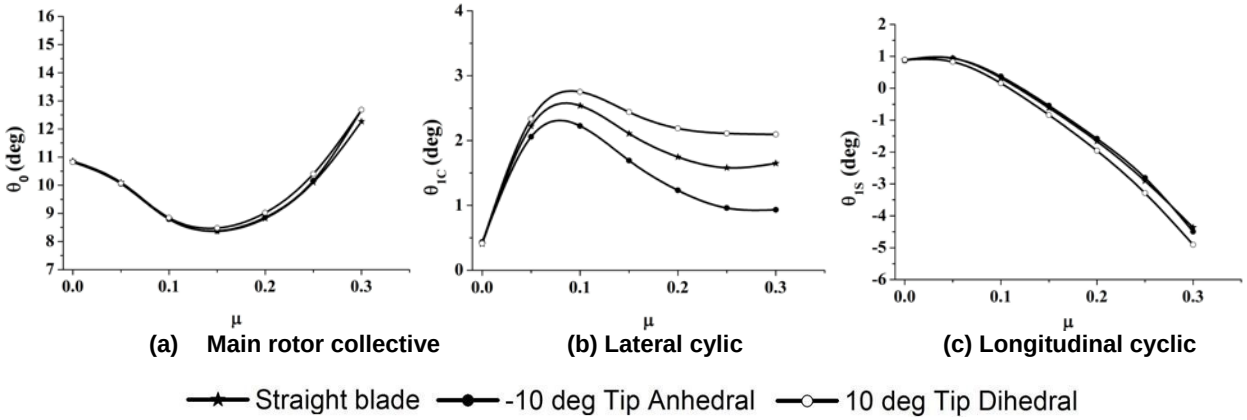

(a) Main rotor collective (b) Lateral cylic (c) Longitudinal cyclic

Fig. 9 Effect of tip-anhedral/dihedral on trim variables

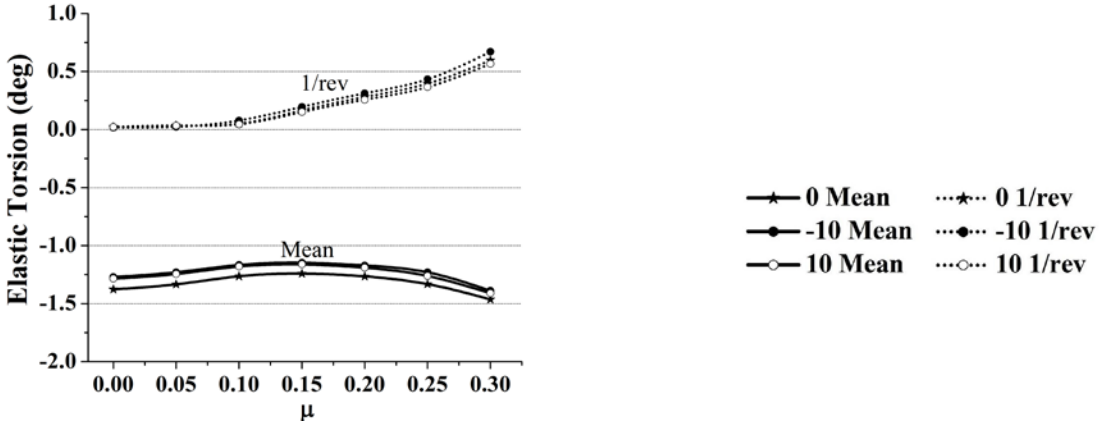

Fig. 10 Blade elastic twist at 0.70R

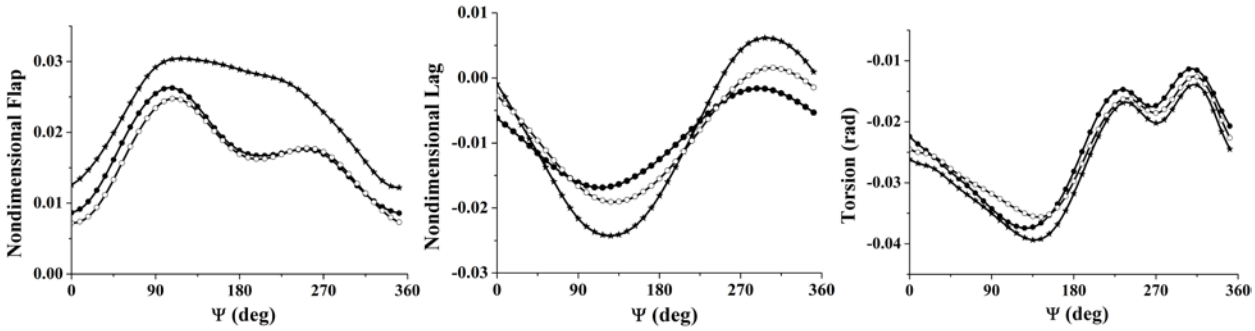

(a) Flap (b) Lag (c) Torsion

Fig. 11 Tip Response at 0.70R for μ = 0.30

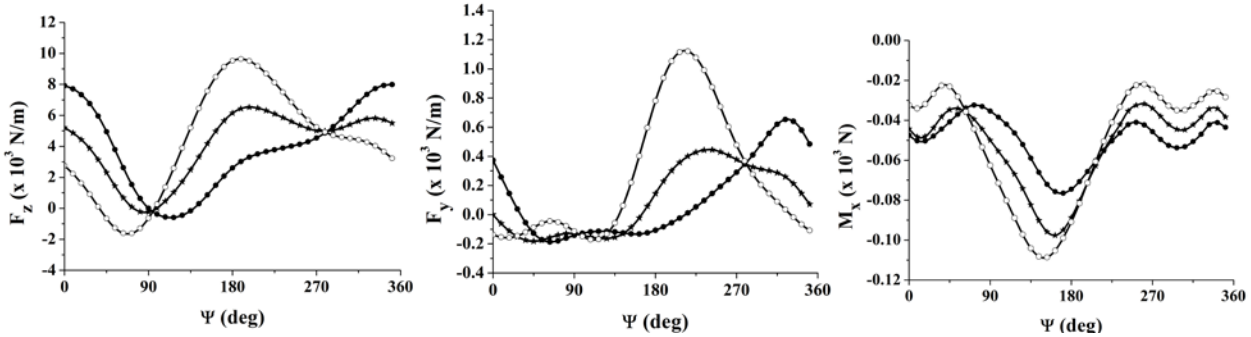

(a) Lift (b) Drag (c) Pitching Moment

Fig. 12 Sectional loads @ 0.95R at μ = 0.30

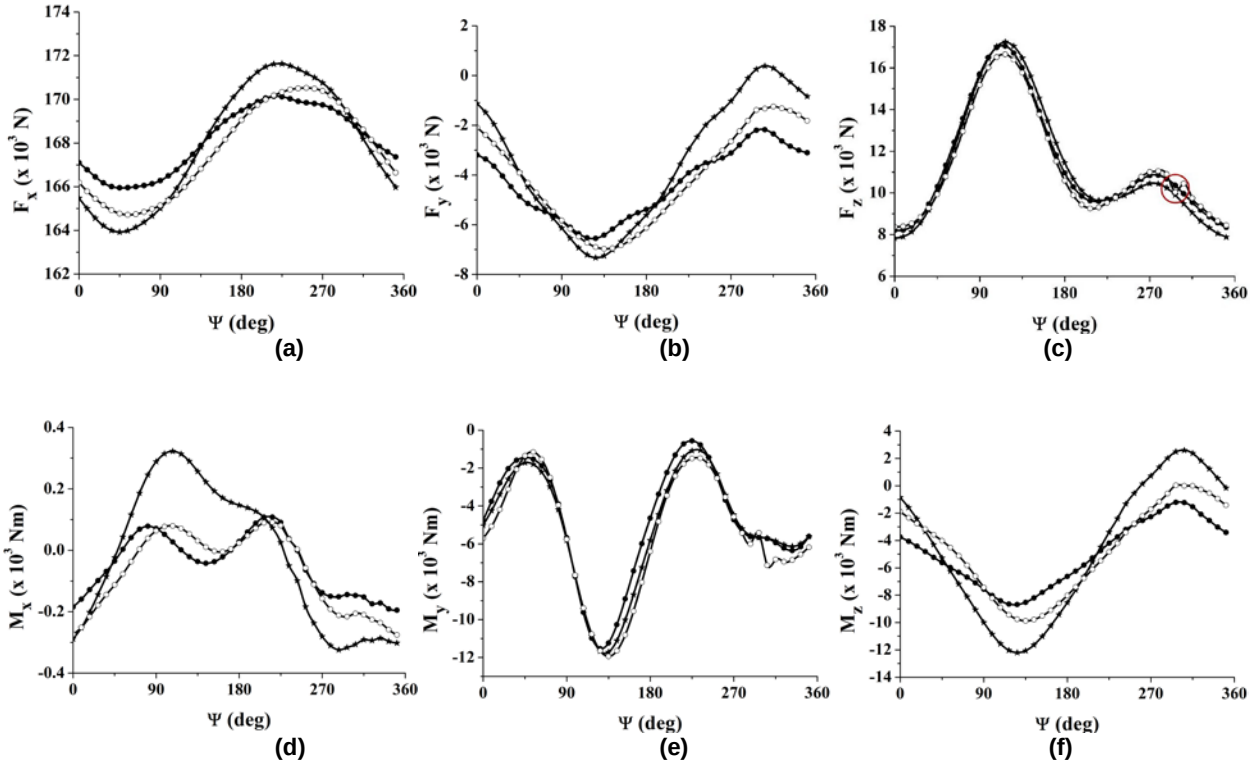

Fig. 13 Root forces and moments at μ = 0.30

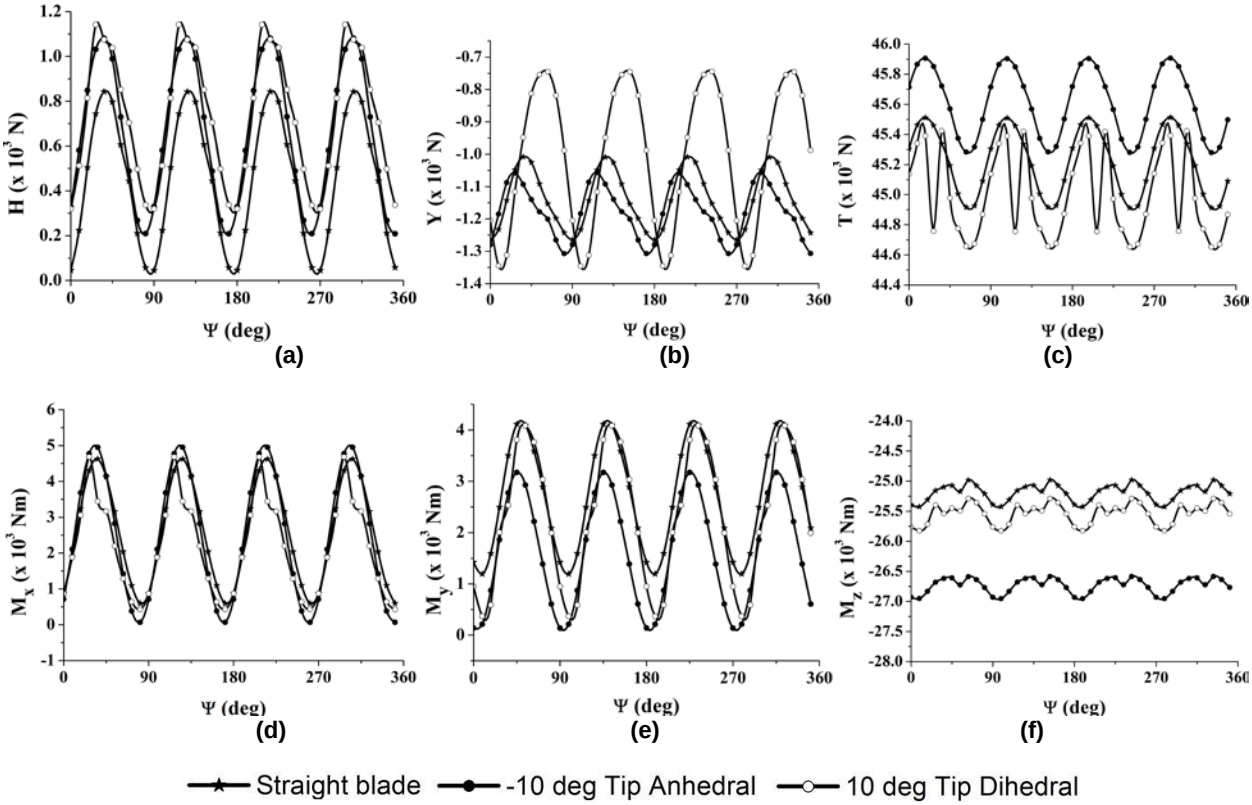

Fig. 14 Hub forces and moments at μ = 0.30

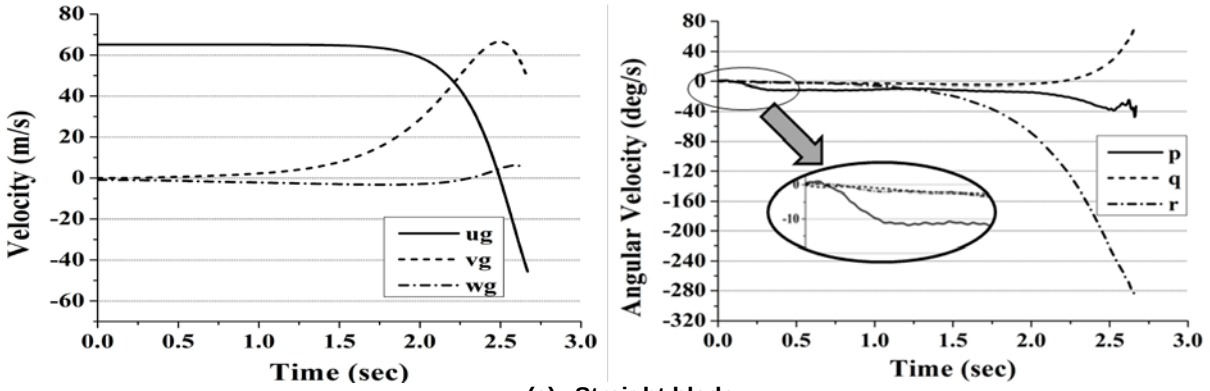

(a) Straight blade

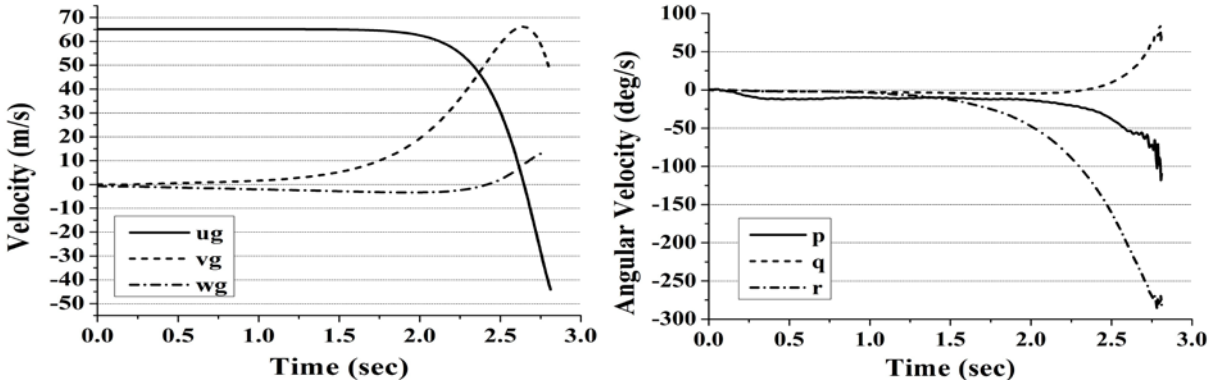

(b) Blade with 30deg tip-sweep

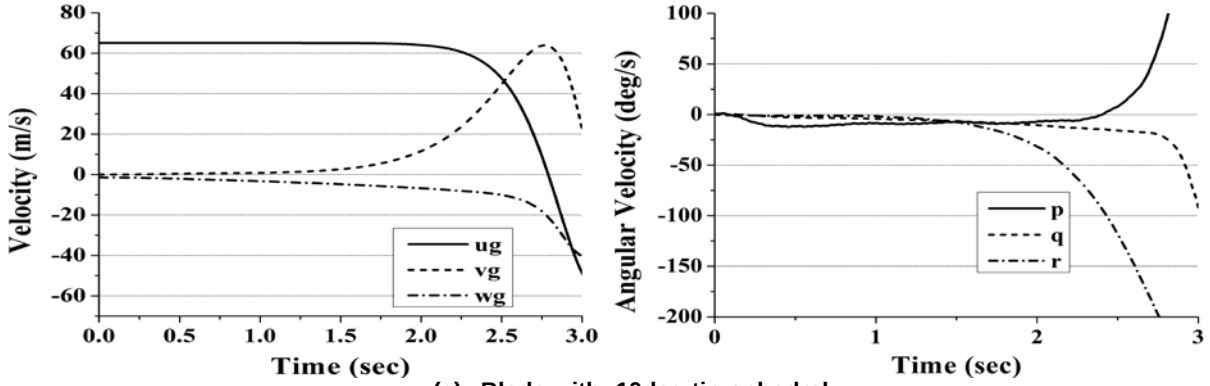

(c) Blade with -10deg tip-anhedral

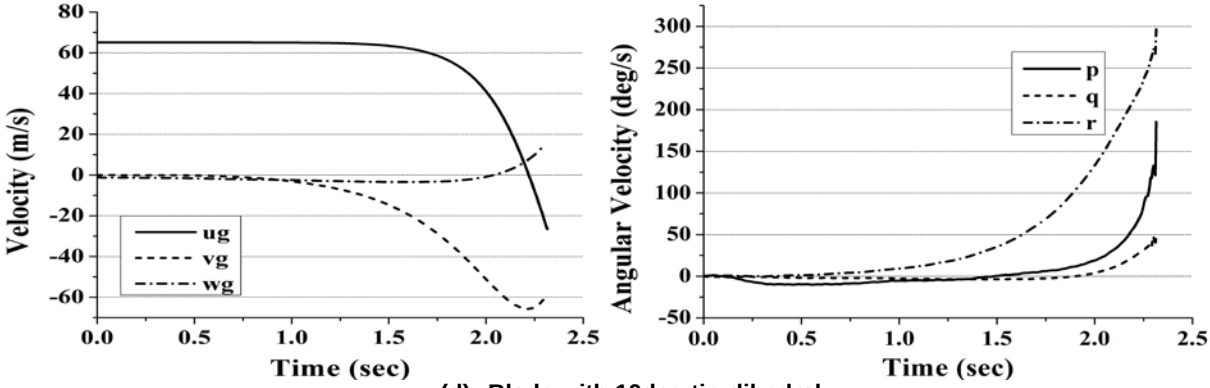

(d) Blade with 10deg tip-dihedral

Fig. 15 Variation of translational and angular velocities for lateral cyclic step-input @ μ=0.30

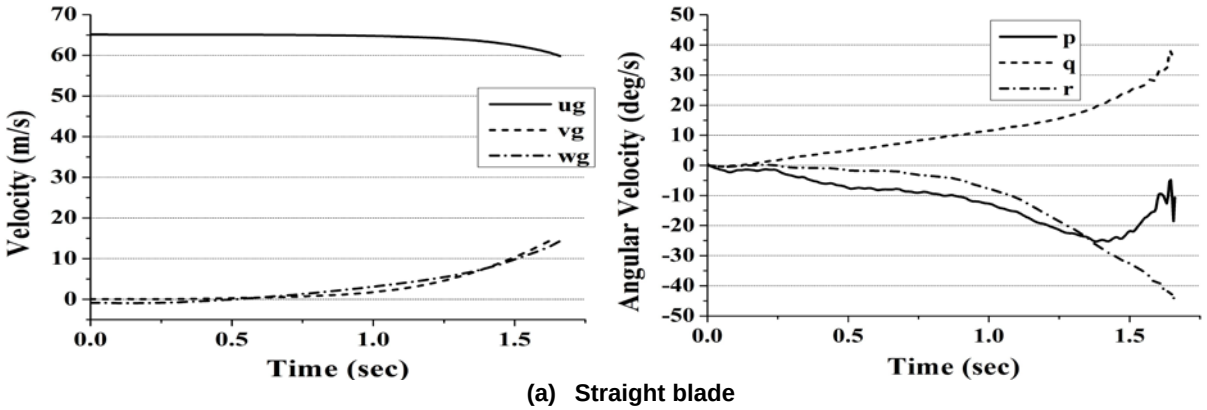

(a) Straight blade

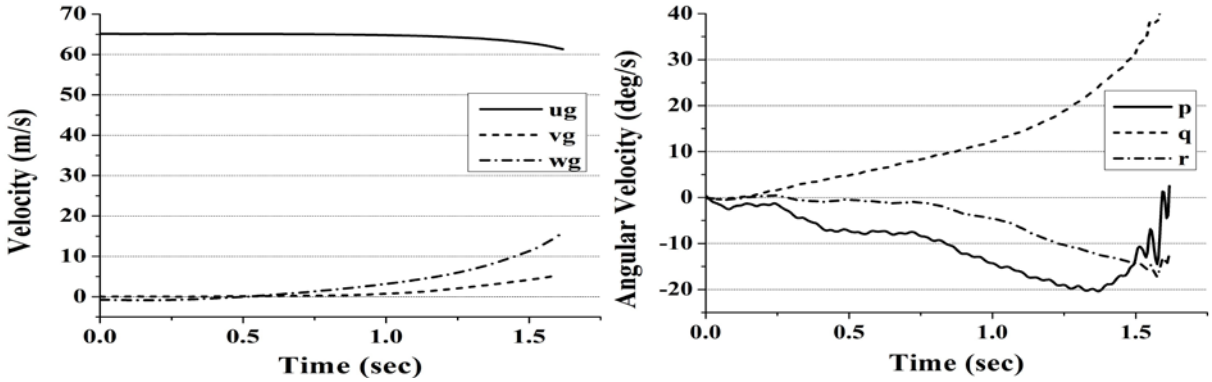

(b) Blade with 30deg tip-sweep

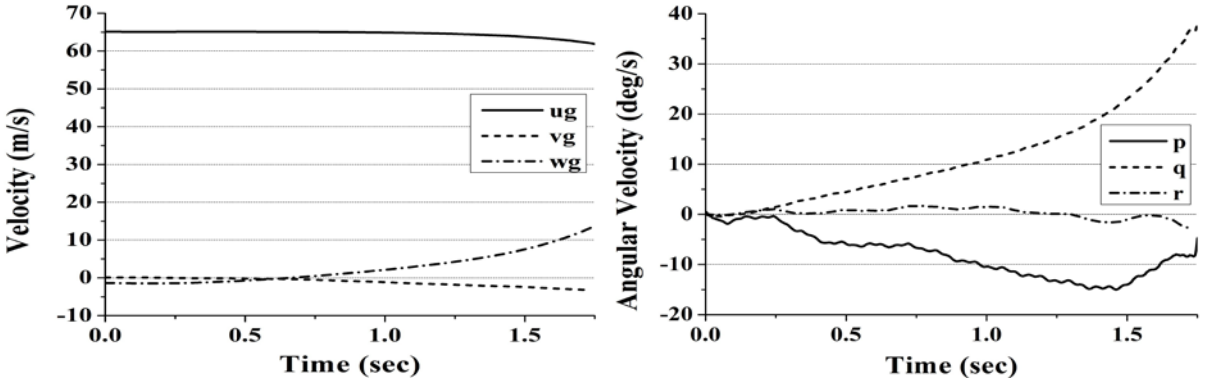

(c) Blade with -10deg tip-anhedral

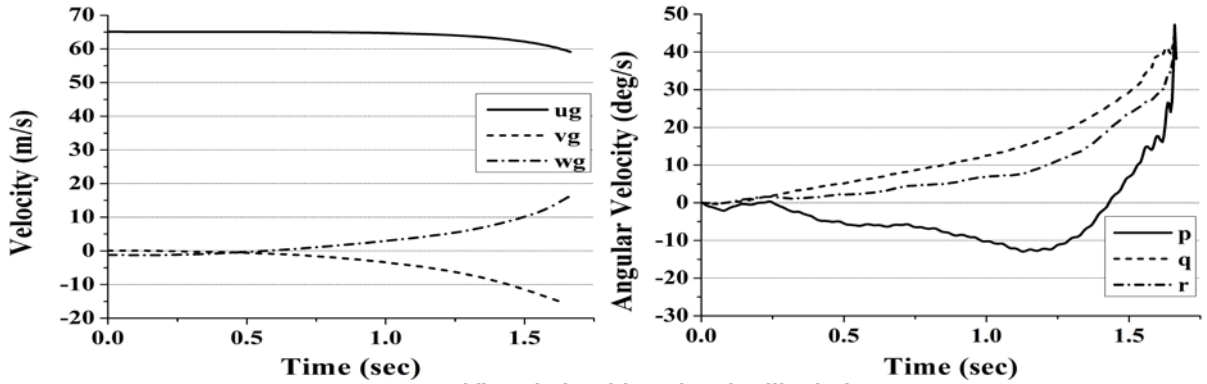

(d) Blade with 10deg tip-dihedral

Fig. 16 Variation of translational and angular velocities for longitudinal cyclic step-input @ μ=0.30